A SEVEN-BEND-ACHROMAT LATTICE AS A POTENTIAL UPGRADE FOR THE ADVANCED PHOTON SOURCE*

M. Borland†, V. Sajaev, Y.-P. Sun, ANL, Argonne, IL 60439, USA

Abstract

The Advanced Photon Source (APS) is a 7-GeV storage ring light source that has been in operation since 1996. In that time, the emittance has dropped from 8 nm to 3 nm. The increasing feasibility of multi-bend-achromat lattices (e.g., the MAX-IV project) promises the possibility of a much greater reduction in emittance. In this paper, we show the design of a symmetric seven-bend-achromat lattice, including linear optics, nonlinear dynamics optimization, magnet requirements, and performance with errors.

INTRODUCTION

There is now wide-spread interest in multi-bend achromat lattices as a means of achieving significantly lower emittance in light source storage rings. Notable efforts include the MAX-IV [1] and SIRIUS projects [2], which are under construction, as well as proposed upgrades for ESRF and SPring-8. A recent report of the Basic Energy Sciences Advisory Committee recommended re-examination of existing upgrade plans for US storage rings to explore the potential of such a lattice. Such work was already on-going at the Advanced Photon Source (APS), but has now taken on renewed urgency.

We have explored a number of lattice concepts, including designs similar to the one being built at MAX-IV. In this paper, we present a design based on the hybrid-multi-bend achromat (HMBA) concept proposed by ESRF [3].

LATTICE OPTIMIZATION

The HMBA lattice is distinguished from the MAX-IV-style lattice by having a dispersion bump between the outer pairs of dipoles, which also feature a longitudinal gradient. Sextupoles are located only in the dispersion bump, by virtue of which their strengths are dramatically reduced. In addition, the phase advance between pairs of sextupole centers in the two dispersion bumps for any sector is 3π and π for the horizontal and vertical planes, respectively.

We started with a lattice file provided by N. Carmignani of ESRF. The first step was to modify the angles for a 40-sector ring (ESRF has only 32 sectors) and perform some basic matching to get a stable lattice. This gave acceptable dynamic acceptance (DA) and local momentum acceptance (LMA), albeit in the absence of errors, and an emittance of about 80 pm at 6 GeV.

For further development, our goal was to reduce the emittance as far as possible, consistent with workable lifetime and sufficient injection aperture for on-axis, swap-out injection [4]. Toward this end, we performed a wide-ranging scan of the integer and fractional tunes that covered over 4000 possible working points with $\nu_x : (99, 109)$ and $\nu_y : (32, 39)$. For each target working point, we used `elegant` [5] to perform linear optics optimization to minimize the emittance, obtain relatively small < 3 m beta functions at the insertion devices (IDs), restrain the maximum beta functions below 20 m, ensure the correct phase advance between sextupoles, ensure the correct overall geometry, etc. In this process, essentially every parameter of the lattice was allowed to vary, including strengths, lengths, and positions of all elements.

Once matching was completed, we corrected the chromaticity to $+2$ in both planes, using a reflection- and translationally-symmetric sextupole distribution. We then used `Pelegant` [6] to perform tracking without errors to determine the maximum stable amplitudes for momentum and amplitude deviations, which involved evaluation of particle survival, crossing of integer and half-integer resonances, and diffusion rates. Figures 1 and 2 show maps of natural emittance and minimum LMA. Note that the latter is often limited at the high-dispersion point and may be smaller than indicated by the tunes vs momentum offset. Figures 3 and 4 show maps of the beta functions at the IDs, which would ideally both be 1.5 m to maximize brightness.

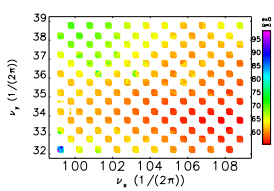

Figure 1: Map of natural emittance vs working point.

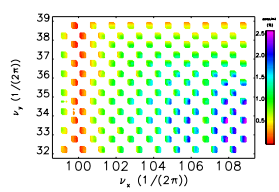

Figure 2: Map of minimum momentum acceptance vs working point.

Since not all parameters can be simultaneously optimized, we performed a non-dominated sort [7], which yielded a handful of superior solutions from which to choose. Dynamic acceptance (DA) and lifetime were optimized for several of these using a tracking-based multi-objective genetic algorithm (MOGA) [8]. This included fine adjustment of the working point and linear optics, as well as adjustment of individual sextupoles. Following ESRF, we organized the sextupoles into 12 families with

* Work supported by the U.S. Department of Energy, Office of Science, under Contract No. DE-AC02-06CH11357.

† borland@aps.anl.gov

ISBN 978-3-95450-138-0

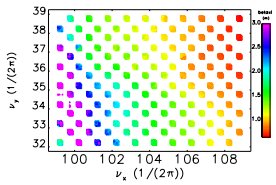

Figure 3: Map of $\beta_{x,ID}$ vs working point.

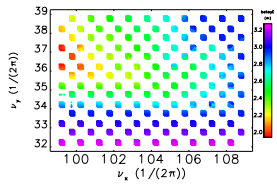

Figure 4: Map of $\beta_{y,ID}$ vs working point.

two-period translational symmetry. Figure 5 shows the lattice functions for the best configuration, while Table 1 lists lattice properties. Of particular note is the natural emittance, which is below 60 pm, and the rather small beta functions at the IDs in both planes. Quadrupole strengths are under 80 T/m, while sextupoles have $|B''| < 6.5kT/m^2$. In the remainder of this paper we present detailed results for this configuration.

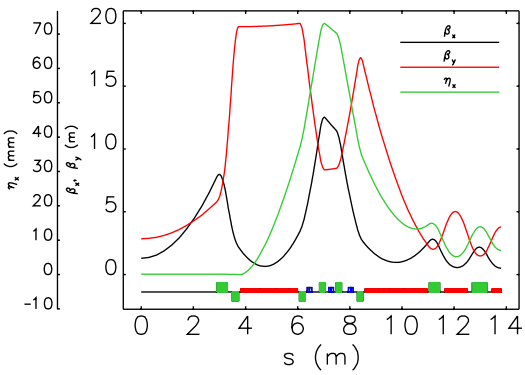

Figure 5: Lattice functions for a half cell, with the ID straight on the left.

Table 1: Parameters of the Optimized Lattice

$\nu_x = 105.45$	$\nu_y = 34.15$
$\epsilon_0 = 59$ pm	$\sigma_{\delta,0} = 0.094\%$
$U_0 = 2.1$ MeV/turn	$\alpha_c = 6 \times 10^{-5}$
Max. $\beta_x = 12.5$ m	Max. $\beta_y = 20$ m
Max. $\eta_x = 73$ mm	
$\beta_{x,ID} = 1.3$ m	$\beta_{y,ID} = 2.9$ m
$\tau_x = 13.5$ ms	$\tau_\delta = 15$ ms

NONLINEAR DYNAMICS

Figures 6 and 7 show the results of frequency map analysis (FMA). We see that the horizontal tune shift with amplitude is quite large. As we'll see below, the regions of the frequency map with no data (e.g., around x=0.5 mm) correspond not to particle loss, but to difficulty determining the tune of the particle when it starts near the $\nu_x = 0.5$ resonance. Detailed simulations with errors showed no particle loss resulting from this resonance. The momentum-dependent tunes and FMA are shown in Figures 8 and 9. Here again we see voids in the FMA resulting from particles with hard-to-determine tunes, not particle loss.

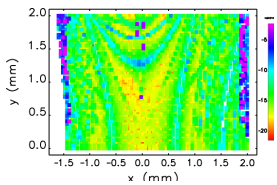

Figure 6: FMA in x-y space.

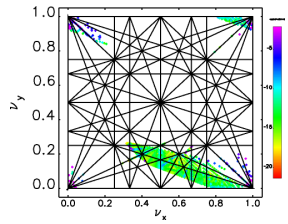

Figure 7: FMA in ν_x-ν_y space.

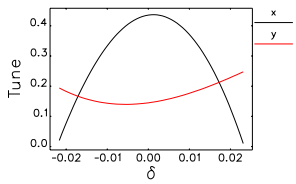

Figure 8: Tunes versus momentum offset.

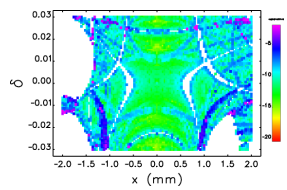

Figure 9: FMA in x-δ space.

For further evaluation, we need a set of error ensembles. We constructed these by first computing lattice functions and 6D equilibrium beam moments for 12,000 ensembles, then selecting those with beta beats between 7 and 10% and $\kappa = \epsilon_y/\epsilon_x : [0.1, 0.2]$. This resulted in 93 ensembles that represent possible machine instances with somewhat large uncorrected errors. We also added systematic multipoles to the quadrupoles and dipoles, at a level of 1% per multipole at a 10-mm radius. Performance with these large errors provides a stringent test of the robustness of the lattice.

DA simulations, shown in Figure 10, exhibit a dynamic aperture of $|x| > 1.3$ mm and $|y| > 1.7$ mm, more than adequate for on-axis injection given that the beam size from the booster will have $\sigma_x = 0.2$ mm and $\sigma_y = 0.3$ mm. The DA search algorithm included radiation damping and had a sufficiently small step size to ensure that the $\nu_x = 0.5$ resonance would not be stepped over. To further verify this, we tracked particles clustered around $x = 0.625$ mm, corresponding to a shift tune bracketing $\nu_x = 0.5$ for each of the 93 ensembles. In tracking for 1500 turns with damping and quantum excitation, no particles were lost, even though many were observed to move across the resonance. Evidently, the tune shift with amplitude is so large that this resonance is not harmful.

Local momentum aperture (LMA) was determined for the 93 ensembles, and is shown in Figure 11. The 10^{th} percentile aperture is over $\pm 2\%$, an acceptable result.

Again, owing to the voids in the FMA shown in Figure 9, we performed additional tracking to verify that the LMA search algorithm did not step over any aperture limits. This consisted of tracking 4100 turns (one longitudinal damping

time) with an 91x91 grid of particles with $x : [-2, 2]$ mm and $\delta : [-4, 4]$ %. A 2-d histogram of the accepted particles for 16 error ensembles, shown in Figure 12, shows the expected region of stability for off-momentum particles.

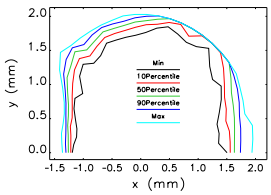

Figure 10: DA contours from 93 error ensembles.

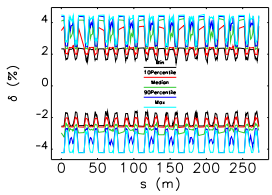

Figure 11: LMA for 93 ensembles, showing 25% of the ring.

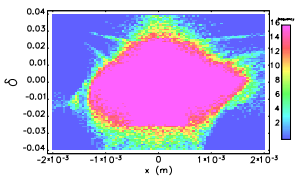

Figure 12: Grid of acceptance counts for 16 error ensembles.

INTRA-BEAM SCATTERING AND LIFETIME

We used `ibsEmittance` [9] to compute the effect of intrabeam scattering (IBS) for two bunch patterns at 200 mA, as a function of the emittance ratio, including a third-harmonic cavity that increases the rms bunch length to 20 mm. Figure 13 shows the effect on the horizontal emittance, which is fairly modest for $\kappa > 0.2$. The effects on energy spread are also modest.

Using the beam parameters from the IBS calculations, we computed the Touschek lifetime using `touscheckLifetime` [10] for the same two bunch patterns. This was done using the 93 LMA results described above, along with the ideal lattice functions. The results, shown in Figure 14, indicate that lifetime for $\kappa = 1$ is 40-60% longer than the lifetime for $\kappa = 0.2$. The gas-scattering lifetime was computed from the DA and the average beta functions listed above using the Toolkit for Accelerator Physics on Androids (TAPAs) [11]. The value is 32 hours, assuming a gas pressure of 2 nT and a gas mixture similar to that found in the APS today.

Since swap-out injection is envisioned, the required lifetime τ with N_b bunches is determined by the minimum possible bunch-swapping interval ΔT_s and the allowed droop $D = N_b \Delta T_s / \tau$ between swaps. With $N_b = 48$, $D = 0.1$, and $\Delta T_s \geq 5$ s, we need $\tau \geq 0.6$ h, which appears possible. For $N_b = 48$, the bunch charge is 15 nC, requiring a rather modest average current of 3.8 nA into the existing accumulator ring, assuming 80% overall efficiency. Accumulation of the required high-charge bunches is described in [12], while the swap-out injection scheme is described in [13].

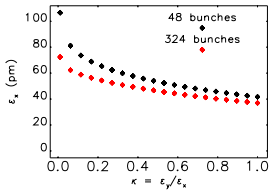

Figure 13: Effect of IBS on the horizontal emittance for 200 mA.

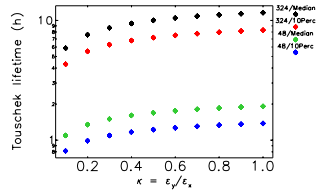

Figure 14: Median and 10^{th}-percentile Touschek lifetime for two bunch patterns.

CONCLUSIONS

A hybrid seven-bend achromat lattice has been developed that could replace the existing APS storage ring, providing a reduction in emittance from 3.1 nm to about 60 pm. Nonlinear dynamics was optimized using a tracking-based multi-objective algorithm, resulting in a design that appears workable for on-axis injection even in the presence of rather large errors. Intra-beam scattering does not have a dramatic effect for emittance ratios greater than about 0.2, even for 48 bunches in 200 mA. Lifetime appears to be workable with the existing APS injector.

ACKNOWLEDGMENTS

Parts of this work were performed using the Blues cluster at Argonne's Laboratory Computing Resource Center and the Mira cluster at Argonne's Advanced Leadership Computing Facility. Thanks to P. Raimondi, L. Farvacque, N. Carmignani, and others at ESRF for providing a copy of an earlier version of their lattice, which helped start this effort.

REFERENCES

[1] S. C. Leemann et al. *Physical Review ST Accel Beams*, 12:120701 (2009).

[2] L. Liu et al. *Proc. IPAC 13*, 1874 (2013).

[3] L. Farvacque et al. *Proc. of IPAC13*, 79 (2013).

[4] L. Emery et al. *Proc.of PAC 2003*, 256 (2003).

[5] M. Borland. ANL/APS/LS-287 (2000).

[6] Y. Wang et al. *ICAP 2009*, 355 (2009).

[7] K. Deb et al. *IEEE TEC*, 6:182 (2002).

[8] M. Borland et al. ANL/APS/LS-319, APS (2010).

[9] A. Xiao. *Proc. Linac 08*, 296–299 (2008).

[10] A. Xiao et al. *PAC 2007*, 3453–3455 (2007).

[11] M. Borland. *Proc. NA-PAC 13*. THPMA06, to be published.

[12] C.-Y. Yao et al. *Proc. NA-PAC 13*. TUPMA03, to be published.

[13] A. Xiao et al. *Proc. NA-PAC 13*. WEPSM13, to be published.

ISBN 978-3-95450-138-0